Pitch Motion Analysis of Vehicles with Trailing-Arms Suspension System

Gianluigi Figliolini and Chiara Lanni

Abstract The subject of this paper is the pitch motion analysis of vehicles with trailing-arms suspension system. In particular, the case of vehicles with braked wheels, where each one is supposed to be locked with respect to its corresponding trailing arm, is considered, while each rigid wheel rolls without sliding on the horizontal supporting plane. Referring to a longitudinal planar sketch of the vehicle, each center point of the two moving revolute joints connecting the two trailing arms with the chassis, will trace an elongated or prolate cycloid path. Consequently, the chassis-link will perform a general planar motion according to an instantaneous equivalent four-bar linkage, which is derived by connecting both centers of curvature of the corresponding moving revolute joint centers, with proper links of variable lengths. Therefore, a specific algorithm is proposed and first numerical and graphical results are proposed. This pitch motion analysis is useful to analyze the vehicle mass center path, along with the dynamical effects of the inertial transfer load during the vehicle sudden breaking and moreover, for designing suitable trailing-arms suspension systems.

1 Introduction

Vehicle dynamics deals with the study of the vehicle behavior in terms of han-dling, braking, ride comfort and stability, according to the wheel-ground interaction, which is fundamental for a correct and safe control. Among this wide category, four-wheel vehicles are of particular interest, since regarding the

---

Gianluigi Figliolini. DIMEAS, Polytechnic of Turin, 10121, Turin, Italy. E-mail: gianluigi.figliolini@polito.it
Chiara Lanni. DICEM, University of Cassino & Southern Lazio, 03043, Cassino, Italy. E-mail: chiara.lanni@unicas.it

quasi totality of car types, but also a lot of wheeled mobile robots and some planetary rovers. It is not so far that the vehicle dynamics has become a distinct science with respect to the dynamics of mechanisms and machines, even if important reference books can be already found since some decades, such as [1-3]. This wide area of competence and research includes many specific topics, but particular attention is devoted to the analysis and design of different suspension system types, both in terms of mechanisms, which connect the single wheel or axle to the vehicle chassis, and also to the whole system including the spring and the shock adsorber [4]. In the same context, wheeled mobile robots are becoming more popular in the last years due to their applications in industrial automation, logistics, inspection, service delivery, and even areas like agriculture and space exploration. A recent review on the wheeled mobile robots state of art can be found in [5], while the design and simulation of a four-wheeled rover is reported in [6]. In fact, one of the major challenges for all-terrain rovers is their ability to main-tain the longitudinal and lateral stability of the platform and these performances can be obtained through a suitable design of the suspension system. Among several types of independent suspension mechanisms, as reported in [1-4], the trailing-arm repre-sents a simple and effective technical solution, since less invasive in terms of size and space occupied, as reported in [7, 8]. One fundamental application of trailing-arms suspension system in passenger cars is represented by the Citroën 2CV, which holds historical importance in the automotive world. For the same motivations, trailing-arms suspension systems find numerous applications also in the field of mobile ro-botics and rovers for the interplanetary exploration.

In this wide context and referring to the fundamentals of kinematics, as detailed in [9], and to what studied in [10,11], the present paper deals with the pitch motion analysis of vehicles with trailing-arms suspension system. Particular attention is devoted to the case of braked wheels, which means to have each wheel and arm locked each other, while every rigid wheel rolls without sliding on the horizontal and rigid supporting plane. Thus, considering what developed in [12] and [13], a specific kinematic model is proposed by formulating the corresponding position analysis with the aim to simulate the vehicle pitch motion in the condition of braked wheels. Afterwards, the curvature analysis is developed with the aid of the prolate cycloid trajectories of both center joint arms and making use of inflection circles. An instantaneous equivalent four-bar linkage is determined in order to substitute both wheel-ground higher pairs with two suitable links and finally, the centrodes of the chassis-link are also determined.

The proposed algorithm has been implemented in a Matlab program and validated through a significant example by showing all the above-mentioned geometric loci in a specific mechanism configuration during the vehicle pitch motion.

2 Kinematic Model and Wheel Motion Analysis

A kinematic model of vehicles with trailing-arms suspension system is sketched in Fig. 1 for the case of a passenger car (Fig. 1a) and a planetary rover (Fig. 1b), which is composed by the rigid flat terrain 1, the front trailing-arm 2 of length a, the chassis-link 3 of length $AB = L$ and the rear trailing-arm 4 of the same length a. Both trailing-arms O_2A and O_4B are attached to the corresponding wheels of centers O_2 and O_4 with radius r, since supposed to be braked. The set-up angle of each trailing-arm is θ_0. Moreover, the wheels-ground contact is supposed to be of pure-rolling, without any sliding, while p is the starting pitch at rest, i.e. under the effect of the total weight, which is vertical and passing through the vehicle mass center G that is located at height h by the midpoint of AB. Thus, the kinematic model is represented by a four-link mechanism, including two higher-pairs with pure-rolling contact at points P_2 and P_4, which take the role of the instant centers of rotation (ICs) for the respective sub-assembly wheel 2 and trailing-arm O_2A, and similarly, for the wheel 4 and trailing-arm O_4B. The vehicle pitch motion in the condition of fully braked wheels 2 and 4, along with their pure-rolling contact on the rigid flat terrain 1, is determined by the movement of the proposed four-link mechanism of Fig. 1, which shows one degree-of-freedom (d.o.f.) and where the chassis-link 3 performs a coupler motion in the vertical plane.

Consequently, each of wheels 2 and 4 executes a cycloidal rigid body motion on the flat terrain 1, while the coupler points A and B will trace two identical, but out of phase, prolate cycloids, since installed outside of the corresponding circles at distance a by their centers O_2 and O_4. This prolate cycloid is sketched in Fig. 2a, along with their corresponding closed-loop vectors, which are referred to the fixed OXY and moving $\Omega\xi\eta$ frames, having the X-axis along the supporting plane profile and the origin Ω coinciding with the wheel center O_2, respectively. At the starting position, which is given by the clockwise angle θ_2 equal to zero, the η-axis is supposed to be coincident with the corresponding Y-axis and consequently, the wheel 2 instant center P_2 coincides with the origin O of the fixed frame. Of course, during this cycloidal pure-rolling motion, the IC P_2 will trace the horizontal straight fixed centrode, along the X-axis, and simultaneously, the moving centrode coinciding with the wheel circle and thus ensuring their tangency at P_2. Therefore, referring to Fig. 2a, the trajectory of the point A is determined by using the following closed-loop equation

$$\mathbf{OA} = \mathbf{OP}_2 + \mathbf{P}_2\mathbf{\Omega} + \mathbf{\Omega A} \tag{1}$$

where $\mathbf{OA}$ is the position vector of A with respect to OXY and likewise, vectors $\mathbf{OP}_2$, $\mathbf{P}_2\mathbf{\Omega}$ and $\mathbf{\Omega A}$ define the alternative path to reach the same point. Each of these vectors can be easily expressed in Cartesian form with respect to OXY by giving **OA** as follows

$$\mathbf{OA} = \mathbf{r}_A = \left(r\theta_2 - a\sin\theta_2\right)\mathbf{i} + \left(r - a\cos\theta_2\right)\mathbf{j} \tag{2}$$

This vector function of the parameter θ_2, depending by the sizes r and a, represents the equation of the point A trajectory, which can be proven to be a prolate cycloid.

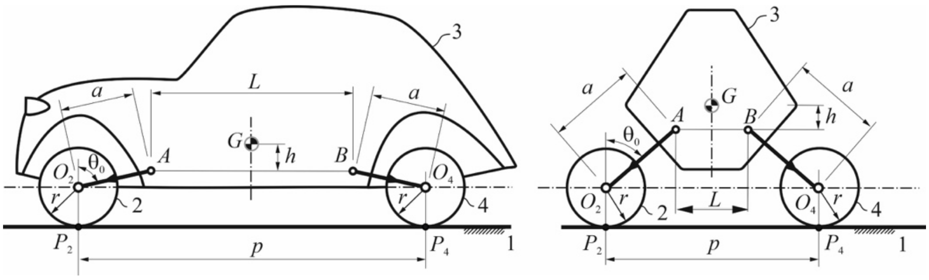

a) b)

Fig. 1. Kinematic model of vehicles with trailing-arms suspension system: a) passenger car; b) planetary rover.

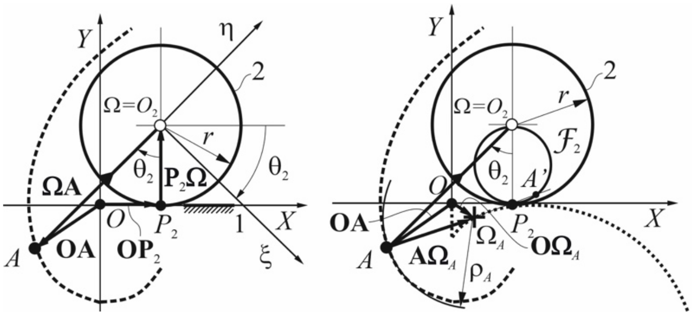

a) b)

Fig. 2. Wheel cycloidal motion: a) trajectory or prolate cycloid; b) evolute or curtate cycloid.

Of course, the same result can be obtained for the coupler point B, as attached to wheel 4 and its corresponding trailing-arm, even if points A and B will trace during the vehicle pitch motion, different arcs of prolate cycloids that are out of phase.

3 Wheel motion: Curvature analysis

Referring to Fig. 2b, the evolute of the trajectory of the point A (prolate cycloid), as the locus of the corresponding centers of curvature, is determined by using the following closed-loop equation

$$\mathbf{O\Omega}_A = \mathbf{OA} + \mathbf{A\Omega}_A \tag{3}$$

where $\mathbf{O\Omega}_A$ is the position vector of the center of curvature Ω_A for the coupler point A with respect to OXY, while $\mathbf{OA}$ and $\mathbf{A\Omega}_A$ are the position vector of A and that of Ω_A with respect to A, supposing to know the radius of curvature ρ_A of A. Thus, referring to the fundamentals of the differential geometry, ρ_A that is also the magnitude of $\mathbf{A\Omega}_A$, can be obtained as follows

$$\rho_A = \frac{\sqrt{\left(\dot{x}_A^2 + \dot{y}_A^2\right)^3}}{\left|\dot{x}_A \ddot{y}_A - \dot{y}_A \ddot{x}_A\right|} \tag{4}$$

where the apices "dot" and "double dot" indicate the first and second derivative of x_A and y_A with respect to the curve parameter θ_2 as Cartesian components of vector $\mathbf{OA} = \mathbf{r}_A$. Correspondingly, one has

$$\dot{\mathbf{r}}_A = \left(r - a\cos\theta_2\right)\mathbf{i} + \left(a\sin\theta_2\right)\mathbf{j} \tag{5}$$

$$\ddot{\mathbf{r}}_A = a\left(\sin\theta_2 \mathbf{i} + \cos\theta_2 \mathbf{j}\right) \tag{6}$$

which components can be substituted into Eq. (4) to give ρ_A. Similarly, and according to the differential geometry, the relative position vector $\mathbf{A\Omega}_A$ can be expressed as

$$\mathbf{A\Omega}_A = \left(\dot{y}_A \frac{\dot{x}_A^2 + \dot{y}_A^2}{\dot{y}_A \ddot{x}_A - \dot{x}_A \ddot{y}_A}\right)\mathbf{i} + \left(-\dot{x}_A \frac{\dot{x}_A^2 + \dot{y}_A^2}{\dot{y}_A \ddot{x}_A - \dot{x}_A \ddot{y}_A}\right)\mathbf{j} \tag{7}$$

Thus, substituting the components of Eqs. (5) and (6) into Eq. (7), and again, substituting the obtained Cartesian form of vector $\mathbf{A\Omega}_A$ into Eq. (3) and developing, one has

$$\mathbf{O\Omega}_A = r\left[\theta_2 + \frac{\sin\theta_2\left(r - a\cos\theta_2\right)}{a - r\cos\theta_2}\right]\mathbf{i} - r\left[\frac{\left(r - a\cos\theta_2\right)^2}{a\left(a - r\cos\theta_2\right)}\right]\mathbf{j} \tag{8}$$

which represents the vector function of the evolute curve (curtate cycloid) of the point A trajectory (prolate cycloid), Of course, the same is true for the other coupler point B.

In alternative and to validate the proposed formulation, the position of Ω_A and the corresponding radius of curvature ρ_A of point A can be determined by using the inflection circle and the Euler-Savary equation. Thus, the diameter Δ_2 of the inflection circle $\mathcal{F}_2$ can be obtained by $\Delta_2 = r_l = r$ where r_λ and r_l are the radii of curvature of the fixed and moving centrodes λ and l, respectively. Of course, considering that λ is a straight line ($r_\lambda \rightarrow \infty$) and l is the circle of radius r, the diameter Δ_2 of the inflection circle $\mathcal{F}_2$ is equal to r, as shown in Fig. 2b in tangency to both centrodes at P_2 IC. Applying the Euler-Savary equation in compact form and making use of the inflection circle, one has

$$(P_2A)^2 = \Omega_A A \cdot A'A \qquad \Omega_A A = (P_2A)^2 / (A'A) \tag{9}$$

where P_2A, $\Omega_A A$ and $A'A$ positive oriented segments and where point A' is the intersecting point of the straight line passing through the points A and P_2, with the inflection circle $\mathcal{F}_2$. Therefore, this geometric construction gives a direct way to evaluate the instantaneous curvature radius ρ_A of the trajectory of point A, as shown in Fig. 2b, since joining the coupler point A, as attached to the moving plane of the wheel 2, with the corresponding P_2 IC, point A' can be easily found. The proposed wheel motion analysis, in terms of both position and curvature, represents the base to define an instantaneous equivalent four-bar linkage and thus for developing the vehicle pitch motion analysis.

4 Vehicle Pitch Motion Analysis

Referring to Fig.3, the position analysis is developed by means of the following closed-loop vector equation

$$\mathbf{OB} = \mathbf{OA} + \mathbf{AB} \tag{10}$$

where **OA** is given by Eq. (2), while the position vectors **OB** and that with respect to A, of point B, are given by

$$\mathbf{OB} = \left[p + r(\theta_0 + \theta_4) - a\sin\theta_4 \right]\mathbf{i} + (r - a\cos\theta_4)\,\mathbf{j} \tag{11}$$

$$\mathbf{AB} = (L\cos\theta_3)\,\mathbf{i} + (L\sin\theta_3)\,\mathbf{j} \tag{12}$$

where θ_3 the oriented angle of vector **AB** with respect to the positive X-axis and θ_4 that defining the orientation of the trailing-arm 4 (O_4B), as shown in Fig. 3.

Thus, substituting the Eqs. (11) and (12) into the Eq. (10) and developing, one has

$$\begin{aligned} &p + r(\theta_0 + \theta_4) - a\sin\theta_4 = r\theta_2 - a\sin\theta_2 + L\cos\theta_3 \\ &r - a\cos\theta_4 = r - a\cos\theta_2 + L\sin\theta_3 \end{aligned} \tag{13}$$

which is a non-linear system of two scalar equations in the two unknowns θ_3 and θ_4, since the geometrical parameters r, L and a, are given, along with the set-up parameters θ_0 and p (starting pitch), while θ_2 represents the driving input angle of the proposed one d.o.f. mechanism that is provided of two higher kinematic pairs in pure-rolling contact.

This non-linear system has been solved by using the *fsolve* function of Matlab, which can give the solution. In particular, the *fsolve* function is able to find all the independent variables, such as those for which all the equations are satisfied. Of course, the choice of the initial mechanism configuration is important to obtain a meaningful result and thus, that of Fig. 1 has been chosen. In order to better understand the vehicle pitch motion in the condition of braked wheels, which are in pure rolling contact with the rigid flat terrain, and with aim to also define an instantaneous equivalent four-bar linkage, the curvature analysis, along with the centrodes, is now formulated by devoting particular attention to the chassis-link motion. Thus, referring to Fig. 3, the inflection circle $\mathcal{F}_3$ passes through the IC P_3 that is determined by applying the Aronhold-Kennedy theorem and thus, as the intersecting point of the two straight lines passing through the ICs P_2 and P_{23}=A, and P_4 and P_{34} = B, respectively. The centers of curvature Ω_A and Ω_B of points A and B, have been determined previously by considering them, as belonging to the respective wheels 2 and 4, by which the instantaneous equivalent four-bar linkage is given by $\Omega_A AB\Omega_B$. In fact, during the vehicle pitch motion, Ω_A and Ω_B are not fixed, but instantaneous moving on the corresponding evolutes, which have the shape of curtate cycloids, as proven before. Coming back to the chassis-link curvature analysis, the positions of the corresponding inflection points A'' and B' of the respective chassis-link coupler points A and B, are determined by applying for each of them, the Euler-Savary equation in the following compact form

$$(P_3A)^2 = \Omega_A A \cdot A''A \qquad A''A = (P_3A)^2 / (\Omega_A A) \tag{14}$$

$$(P_3B)^2 = \Omega_B B \cdot B''B \qquad B''B = (P_3B)^2 / (\Omega_B B) \tag{15}$$

Consequently, the equation of the inflection circle $\mathcal{F}_3$ has been derived by applying the analytical geometry and considering that P_3, A'' and B' are points of $\mathcal{F}_3$.

Afterwards, the position of the center of curvature Ω_G of the vehicle mass center G, along with the corresponding radius of curvature $\Omega_G G$, can be determined as follows

$$(P_3G)^2 = \Omega_G G \cdot G'G \qquad \Omega_G G = (P_3G)^2 / (G'G) \tag{16}$$

where G is the intersecting point with $\mathcal{F}_3$, of the line joining the IC P_3 with G.

These results are useful to analyze trajectory and curvature of G, during the vehicle pitch motion, such as that generated by a sudden braking maneuver, where the inertial load transfer significantly affect the vehicle stability. The chassis-link coupler motion is also analyzed by means of the corresponding fixed λ_3 and moving l_3 centrodes, which are traced by the IC P_3 with respect to OXY and Ax_2y_2 frames, respectively. In particular, λ_3 is given by the position vector $\mathbf{r}_{\lambda 3}$ of P_3 in OXY as function of θ_2. One has

$$\mathbf{r}_{\lambda 3} = \frac{\sin\theta_2\left\{\left[p+r(\theta_0+\theta_4)\right](a\cos\theta_4-r)-a\theta_2\cos\theta_4\right\}+r^2\theta_2\sin\theta_4}{r(\sin\theta_4-\sin\theta_2)+a\sin(\theta_2-\theta_4)}\mathbf{i}+ \\ +\frac{(r-a\cos\theta_2)(r-a\cos\theta_4)\left[p+r(\theta_0+\theta_4-\theta_2)\right]}{ra(\sin\theta_4-\sin\theta_2)+a^2\sin(\theta_2-\theta_4)}\mathbf{j} \tag{17}$$

Similarly, the moving centrode l_3 is given by $\mathbf{r}_{l3}$ of P_3 in Ax_2y_2 and as function of θ_2.

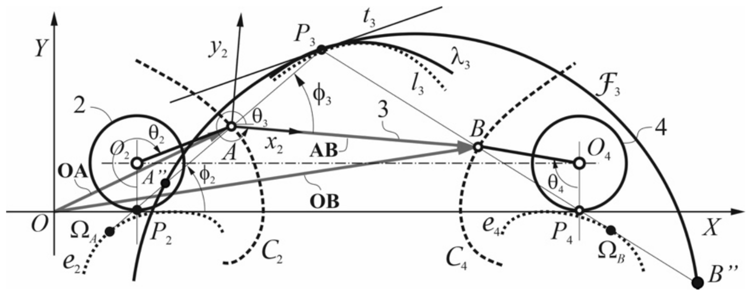

Fig. 3. Vehicle pitch motion analysis: vectors closed-loop, fixed λ and moving l centrodes, along with the inflection circle $\mathcal{F}_3$ of the chassis-link 3.

Thus, one has

$$\mathbf{r}_{l3} = \sqrt{(x_{P3}-x_A)^2+(y_{P3}-y_A)^2}\,(\cos\phi_3\mathbf{i}+\sin\phi_3\mathbf{j}) \tag{18}$$

where x_A, y_A, x_{P3} and y_{P3} are the Cartesian components of the position vectors **OA** and $\mathbf{r}_{\lambda 3}$ of points A and P_3, which are given by the Eqs. (2) and (17), respectively. The oriented angle ϕ_3 of the P_3 position vector $\mathbf{r}_{l3} = \mathbf{AP}_3$ with respect to the x_2-axis, is expressed as $\phi_3 = \phi_2 - 360° + \theta_3$, where ϕ_2 is related to the driving link 2 ($\Omega_A A$) of the proposed instantaneous equivalent four-bar linkage $\Omega_A AB\Omega_B$. Thus, one has

$$\phi_2 = \tan^{-1}\left[(r-a\cos\theta_2)/-a\sin\theta_2\right] \tag{19}$$

Of course, Eq. (18) expresses the moving centrode l_3 with respect to the moving frame Ax_2y_2, but this curve is attached to the chassis-link 3 (AB) by performing the same planar rigid body motion and simultaneously rolling, without slipping, on the corresponding fixed centrode λ_3. More conveniently, this curve can be expressed in the fixed frame OXY, by means of the following homogeneous transformation matrix

$$\mathbf{T}_3 = \begin{bmatrix} \cos\theta_3 & -\sin\theta_3 & x_A \\ \sin\theta_3 & \cos\theta_3 & y_A \\ 0 & 0 & 1 \end{bmatrix} \tag{20}$$

where θ_3 is the counterclockwise angle of $A\,x_2\,y_2$ with respect to OXY, while x_A and y_A are the Cartesian coordinates of A. Multiplying $\mathbf{T}_3$ of Eq. (20) times $\mathbf{r}_{\lambda 3}$ of Eq. (17), in homogeneous matrix form, the moving centrode l_3 is obtained with reference to OXY.

5 Graphical and Numerical Results

The proposed formulation has been implemented in Matlab and validated through significant examples, such as that of Fig. 4, which refers to the case for $\theta_2 = 249°$ (driving input angle), $r = 200$ mm (wheel radius), $a = 450$ mm (trailing-arm length), $L = 1129$ mm (chassis-link length) and $p = 1995$ mm (starting pitch) by which $\theta_0 = 74.4°$. The mechanism configuration of Fig.4 corresponds to a clockwise rotation of both arms O_2A and O_4B, starting from that with $\theta_2 = 245°$, since the total range of θ_2 is 245°-270°.

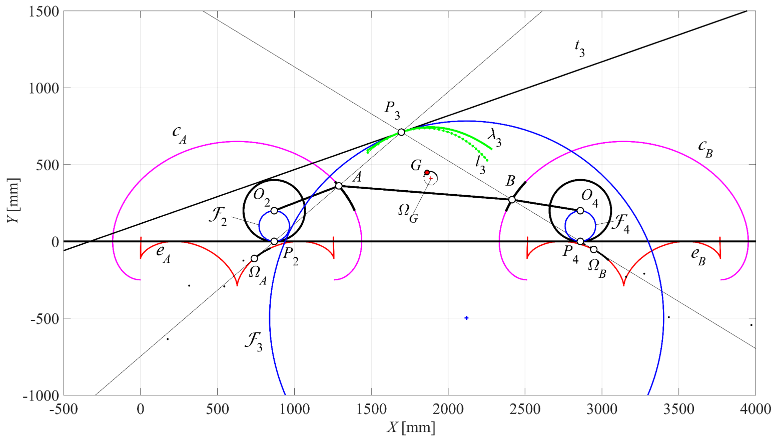

Fig. 4. Pitch motion analysis for a trailing-arms suspension system: results for $\theta_2 = 249°$.

In particular, one can observe a generic configuration of both, the real mechanism with the two pure-rolling higher-pairs, in the form of the two wheels 2 and 4 in contact with the rigid flat terrain 1, along with the instantaneous equivalent four-bar linkage $\Omega_A A B \Omega_B$. Both prolate cycloids c_A and c_B of points A and B, along with their corresponding evolute curves e_A and e_B (curtate cycloids), are shown, respectively.

6 Conclusions

The pitch motion analysis of vehicles with trailing-arms suspension system has been proposed by devoting particular attention to the case of braked wheels in pure-rolling contact with the rigid flat terrain. A specific algorithm has been formulated and implemented in Matlab to analyze the chassis-link pitch motion of the instantaneous equivalent four-bar linkage, which is composed with both trailing arms, locked at the corresponding wheels, and the supporting plane. First numerical and graphical results dealing with centrodes and significant geometric loci, have been presented and discussed.

References

1. Genta, G.: Motor Vehicle dynamics: modeling and simulation. World Scientific Publishing Company, Singapore (1997)
2. Guiggiani, M.: The Science of vehicle dynamics: handling, braking, and ride of road and race cars. 3rd Ed., Springer International Publishing, Cham, Switzerland (2023)
3. Jazar, R.N.: Vehicle dynamics: theory and application. 4th Edition, Springer Int. Publishing, Cham, Switzerland (2025)
4. Reimpell, J., Stoll, H., Betzler, J.W.: The automotive chassis: engineering principles. 2nd Ed., Butterworth-Heinemann, Oxford, U.K. (2001)
5. Ling Leong, J.S., Kin Teo, K.T., Yoong, H.P.: Four wheeled mobile robots: a review. In: IEEE Int. Conf. on Artificial Intel. Eng. and Tech., Kota Kinabalu, Malaysia, pp. 1–6 (2022)
6. Kuncolienkar, A., Panigrahi, S., Asokan, T.: Design and simulation of a four-wheeled rover for enhanced lateral stability. In: 21st Int. Conf. on Adv. Rob., Abu Dhabi (UAE), pp. 446–451 (2023)
7. Gao, J., Qi, X.: Position design of the trailing arm bushing on torsion beam suspension accounting for vehicle transient handling performance and uncertainties. Advances in Mechanical Engineering, vol. 15, n. 9 (2023)
8. Xinbo, C., Yanjia, L., Naiwen X., Xiang X.: Research of parameter optimization of double trailing arm suspension mechanism for integrated wheel side deceleration electric drive system. J. of Physics: Conference Series, vol. 1939, n.1 (2021)

9. Angeles, J., Bai, S.: Kinematics of mechanical systems: fundamentals, analysis and synthesis. Springer, Cham, Switzerland (2022)
10. Lanni, C., Figliolini, G., Tomassi L.: Roll center and centrodes of an eight-bar suspension system. In: Proc. of the ASME 2023 IDETC & CIE in Eng. Conf., Boston (MA), USA, DETC2023-116901 (2023)
11. Lanni, C., Figliolini, G., Tomassi, L.: Kinematic and curvature analysis of the McPherson eight-bar suspension system. In: Proc. of the ASME 2024 IDETC & CIE in Eng. Conf., vol. 48th Mechanisms and Robotics Conf., Washington (DC), USA, V007T07A004 (2024)
12. Figliolini, G., Lanni, C., Tomassi, L.: Synthesis and analysis of Stephenson III six-bar motion generators with an instantaneous stop link. J. of Mech. & Rob., vol. 17, n.4, 044510, (2025)
13. Figliolini, G., Lanni, C., Tomassi, L.: First- and second-order centrodes of both coupler links of Stephenson III six-bar mechanisms. Machines, vol. 13, n. 2, (22 pages), 93, (2025)